Scientific Research Publishing

Open Journal of Modelling and Simulation, 2025, 13(4), 196-203
https://www.scirp.org/journal/ojmsi
ISSN Online: 2327-4026
ISSN Print: 2327-4018

Effect of Stenosis and Aneurysm on Atherosclerotic Hemodynamics during a Blood Pulsatile Flow

Md. Jashim Uddin

Department of Applied Mathematics, Noakhali Science and Technology University, Noakhali, Bangladesh
Email: mdjaud11@gmail.com

How to cite this paper: Uddin, Md.J. (2025) Effect of Stenosis and Aneurysm on Atherosclerotic Hemodynamics during a Blood Pulsatile Flow. *Open Journal of Modelling and Simulation*, **13**, 196-203.
https://doi.org/10.4236/ojmsi.2025.134011

Received: July 15, 2025
Accepted: August 26, 2025
Published: August 29, 2025

Abstract

The danger of rupture for severe cases of stenosis and aneurysms is extensively studied by healthcare professionals and researchers. Numerical researchers have likewise played a role in forecasting this rupture. This study offers a numerical computation of a time-dependent three-dimensional arterial flow of Newtonian fluid, examining the influence of stenosis and aneurysm on atherosclerosis-related hemodynamics. The pulsatile blood flow simulation has been executed with the software code of COMSOL Multiphysics using a finite element approach. Results indicate that the stenotic model creates hemodynamic conditions associated with a higher risk of thrombosis compared to the aneurysm model. A higher viscous stress is found in the stenotic model compared to that of the aneurysm model. Higher magnitudes of velocity and pressure are estimated for the stenotic model. It can be concluded that for the same height of stenosis and aneurysm, the stenosis model poses a severe risk to humans.

Keywords

Stenosis, Aneurysm, Hemodynamics, Atherosclerosis, Pulsatile Flow

1. Introduction

A localized, seditious fibroproliferative reaction to various types of endothelium damage is known as atherosclerotic arterial disorder [1]. During atherosclerotic stage, the buildup and deposition of lipid substances and cholesterol, along with the formation of combinative tissues, result in a fragmental reduction of the artery cross-sectional locality, referred to as stenosis. Conversely, an aneurysm is defined

as a localized expansion of an artery resulting from an acquired or inherited weakness of the wall of vessel. Around the world, cardiovascular illnesses are a major source of morbidity and death. One of the main causes of these disorders is artery stenosis, a disorder in which plaque builds up in the arteries, narrowing them and decreasing blood circulation [2]-[6]. Research on blood circulation within narrowed arteries has garnered considerable attention due to its direct implications for cardiovascular well-being. Numerous factors, including the stenosis's shape, the blood's characteristics, and the existence of disease, affect the extremely complex blood circulation in the aforementioned vessels [7]-[11].

Several studies and computational fluid dynamics (CFD) assessments have been carried out to investigate the flow disruption brought on by human aneurysm formation, leading to cardiovascular disorders [12]-[16]. Narayan *et al.* [17] have analyzed the blood flow in an aneurysm within a magnetic field to evaluate the hemodynamic risk factors. The study has shown that the globular and bilobed forms are more likely to experience sac rupture and lateral neck expansion. Blood pulsation flow has been numerically simulated by Elgar *et al.* [18], who have identified several flow types and examined how they affect hemodynamics. Paramasivam *et al.* [19] have created a program to aid in the diagnosis and management of aneurysms. The current study presents a comparison of stenosis and aneurysm in hemodynamic risk parameters, which is the research gap [20].

This paper aims to examine the hemodynamic conditions within a diseased artery, focusing on a 45% depth related to stenosis and aneurysm models for the analysis. Although a significant amount of research work has been conducted to examine the changes in various parameters in the circulation of blood in various modeled stenoses and aneurysms, no research has been conducted to examine the flow characteristics in terms of hemodynamic risk factors of aneurysms with stenoses of the identical size. The present research offers this numerical investigation.

2. Numerical Methodology

2.1. Model of Simulation

Blood is modeled as a Newtonian fluid because it is a reasonable approximation for flow in large arteries. The two geometric models of stenosis (**Figure 1(a)**) and aneurysm (**Figure 1(b)**) have been taken to examine the mimicked blood flow hemodynamics. The computational domain has features that the lengths of pre-stenosis and post-stenosis areas are 15 mm and 50 mm, respectively. The coordinates X and Y present the direction of horizontal and vertical. The arterial geometry has a radius of 2.5 mm.

2.2. Governing Equations and Boundary Conditions

The equations that govern the continuity and Navier-Stokes are as follows:
The fluid flow's continuity equation is

$$\nabla \cdot \boldsymbol{u} = 0 \tag{1}$$

The Navier-Stokes equation is

$$\rho\left(\frac{\partial \boldsymbol{u}}{\partial t}+(\nabla\cdot\boldsymbol{u})\boldsymbol{u}\right)=-\nabla p+\nabla\cdot\boldsymbol{\tau} \tag{2}$$

where $\boldsymbol{u}$ is the velocity vector, t is the time, ρ indicates the density of the fluid, and p is the fluid pressure. The viscous stress tensor $\boldsymbol{\tau}$ is identified in the following way:

$$\mu\left(\nabla\boldsymbol{u}+(\nabla\boldsymbol{u})^{\mathrm{T}}\right)$$

where the parameter μ presents the dynamic viscosity of the fluid.

The computational fluid domain's inlet takes the following time-dependent velocity pulse [21], as follows:

$$U_{inlet}=50955.4*\left(0.0000043+0.0000026*\sin\left(2\pi t/T\right)\right).$$

No-slip boundary condition is considered across the wall, and the outlet pressure is static.

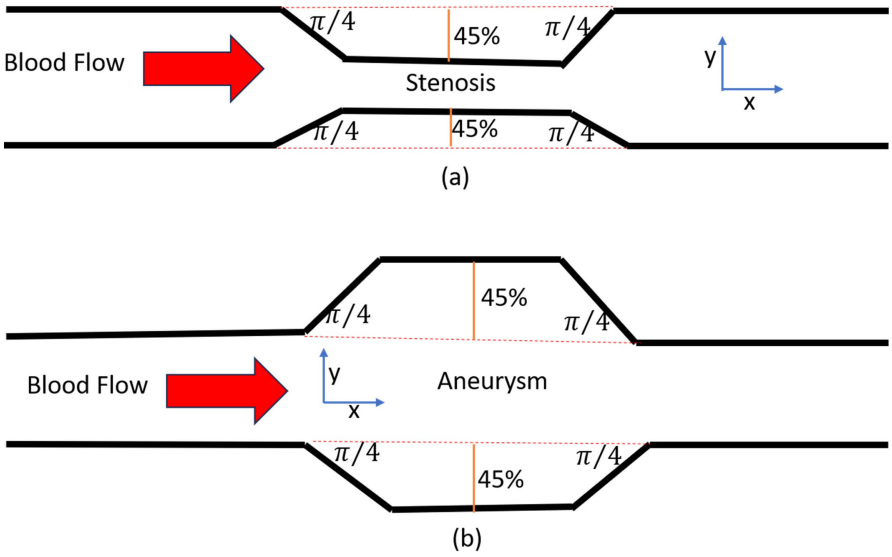

Figure 1. The current simulation model of (a) stenosis and (b) aneurysm.

2.3. Numerical Solution Approach

Computational fluid dynamics is a significant scheme to evaluate the potential outcomes in blood flow investigation. The areas before and after the stenosis are selected to reduce the impact of the boundary conditions of inflow and outflow, and adequately represent the flow characteristics at the downstream region. The finite element scheme-based software code for COMSOL has been employed to capture the simulation outcomes. The selected grid resolution is displayed in Figure 2(a). Figure 2(b) exhibits the grid test for various mesh densities. The mesh elements of 204605 are chosen because the simulation outcomes of time-averaged wall pressure are approximately identical for mesh sizes of 204,584 and 306,554. As the flow is pulsatile, the second cycle has been adopted.

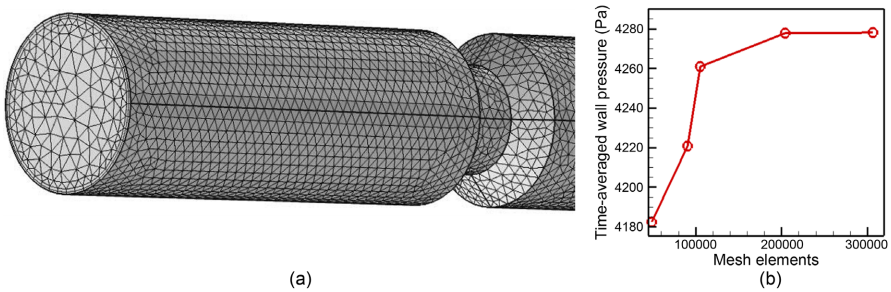

Figure 2. (a) Grid resolution and (b) grid independence test in time-averaged wall pressure.

2.4. Validation

This research validates and confirms the correctness and uniformity of the numerical computational estimation by comparing the results with those of the investigation by Lee *et al.* [22] using axial velocity along the radial coordinate. Furthermore, there is a significant amount of agreement between the present velocity profile and those obtained by prediction Lee *et al.* [22], as displayed in **Figure 3**. Lee *et al.* [22] validate their work with experimental data, so this validation can be claimed as an experimental validation. The axial velocity predicted in a rigid wall at a downstream area (8.6 × radius) for the time point of 0.08625 sec shows good agreement.

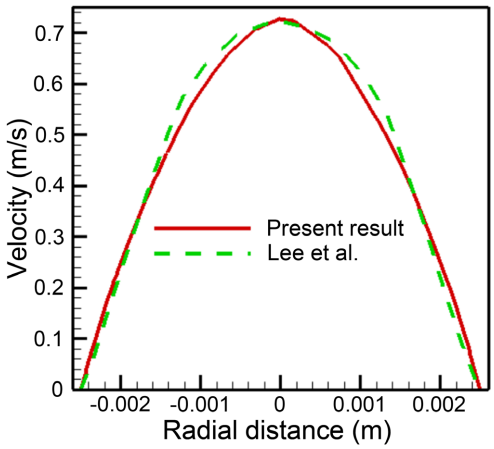

Figure 3. Axial velocity profile is validated with Lee *et al.* [22].

3. Results and Discussion

3.1. Velocity Distribution Due to Stenosis and Aneurysm

In the present research, the pulsating blood flow through stenotic and aneurysm shapes has been modeled by the continuity and Navier-Stokes equations to investigate the influence of variational shapes. **Figure 4** displays the flow disruptions and velocity distributions generated in various sections of the stenotic and aneurysmal shapes with a depth of 45%. The speed is consistently reduced in the area near the wall for both shapes, with this decrease in speed being more significant in stenosis and experiencing a higher velocity than in aneurysm.

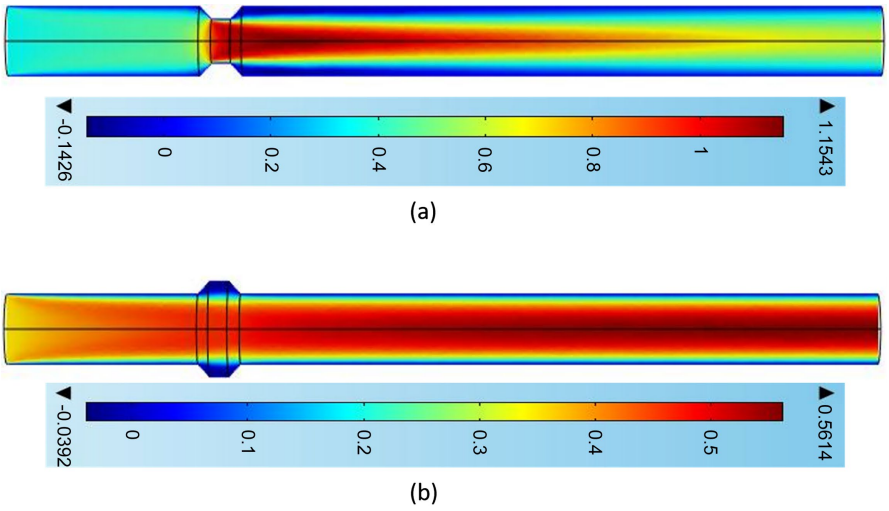

Figure 4. Velocity distribution for (a) stenosis and (b) aneurysm during systolic phase.

3.2. Hemodynamics Bio-Indices' Impact

The time-averaged bio-marker factors, such as time-averaged wall shearing stress (TAWSS), oscillatory shearing index (OSI), and relative residence time (RRT), are displayed axially in Figures 5(a)-(c). It has been noted that, in the case of stenosis, the TAWSS reaches its peak at the stenosis's inlet region since the flow impacts directly on this side, leading to a sudden rise in TAWSS, moderately elevated across the stenosis region, and ultimately declines from the ending sections. However, aneurysm's TAWSS characteristics differ from those observed in stenosis. In this case, the highest TAWSS occurs initially, and after that, it occurs at its highest at the aneurysm's outlet region because the inlet side's flow expands and impacts the ending side, resulting in elevated TAWSS. The highest peaks of OSI and RRT indicate the reattachment points, which correspond to zero for TAWSS. Figure 5(d) presents the WSS contours due to the shapes of stenosis and aneurysm, indicating the highest shear stress at the stenosis location, whereas it reflects the opposite magnitudes of wall shear stress due to the shape of the aneurysm.

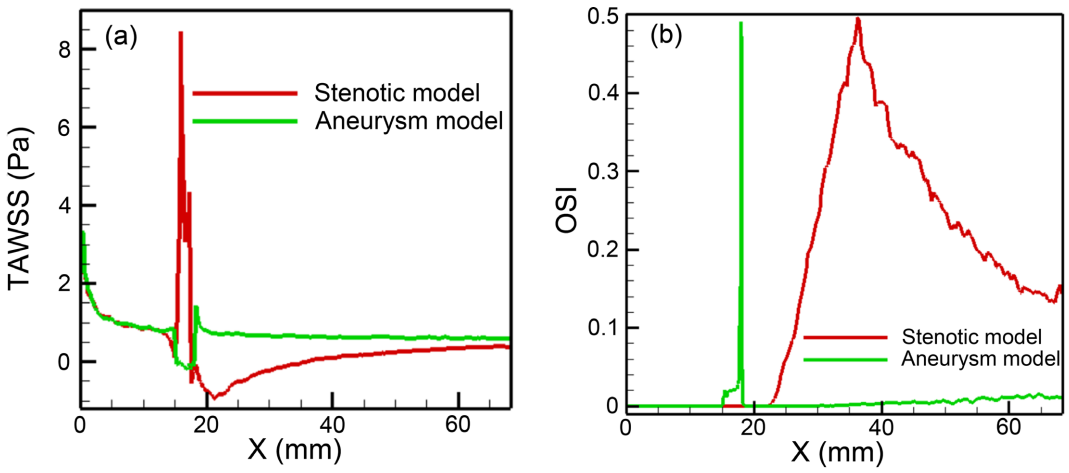

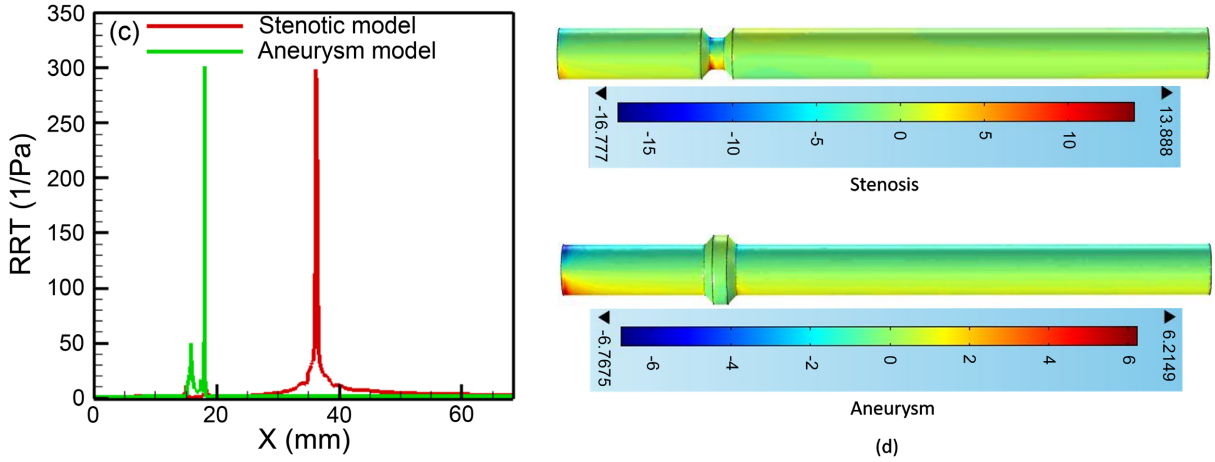

Figure 5. Distributions of (a) TAWSS, (b) OSI, (c) RRT, and (d) contours of WSS, for the models of stenosis and aneurysm.

3.3. Pressure Distribution Contour

The pressure caused by stenosis and aneurysm is a crucial factor in comprehending the critical condition if it is not identified and assessed correctly. In Figure 6, pressure contours for stenosis show that the pressure peaks in the areas before the blockage and decreases at the narrowest point of the stenosis model, leading to minimum pressure at the throat of the blockage. Additionally, the pressure rises within the aneurysm but decreases in the remote downstream areas. The pressure contours in Figure 6 conclusively present that the maximum pressure is attained at its stenosis location for the stenosis model, whereas for the aneurysm model, the lowest pressure is acquired at the post-aneurysmal distal part.

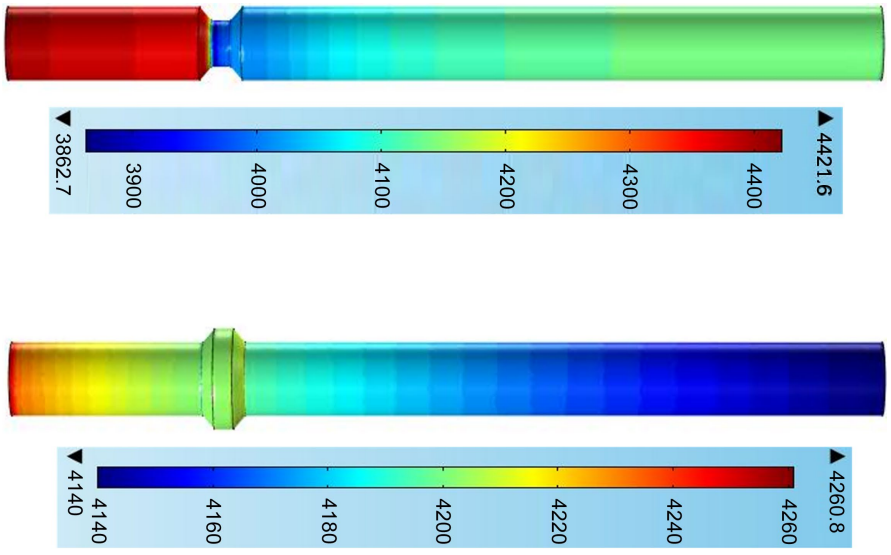

Figure 6. Pressure contours for stenotic model (upper) and aneurysm model (bottom).

4. Conclusions

The current work examines the impact of the laminar flow of pulsation across the arterial stenotic and aneurysmal models using a computational approach of COM-

SOL Multiphysics in three dimensions. The stenosis of the trapezium with the angulation of 45˚ and depth of 45% has been employed to observe the influence on both models. Time-averaged parameters, including TAWSS, OSI, and RRT, are the leading potential risk factors utilized to capture the atherosclerotic recirculation area. The findings show that, in contrast to the aneurysm model, the stenotic model provides the possible danger of a thrombotic area. The stenotic model exhibits a greater viscous stress than the aneurysm model. Greater values of velocity and pressure are predicted for the stenotic model. It can be inferred that for identical heights of stenosis and aneurysm, the stenosis model presents a significant threat to humans. In conclusion, it can be said that the research outcomes may be used in biomedical applications.

Future extensions of this research may focus on patient-specific non-Newtonian models in fluid-structure interaction methods. The results may be applied in bioengineering areas.

Conflicts of Interest

The author declares no conflicts of interest regarding the publication of this paper.

References

[1] George, S.J. and Johnson, J. (2010) Atherosclerosis: Molecular and Cellular Mechanisms. John Wiley & Sons.

[2] Akbar, S. and Shah, S.R. (2024) Mathematical Modeling of Blood Flow Dynamics in the Cardiovascular System: Assumptions, Considerations, and Simulation Results. *Journal of Current Medical Research and Opinion*, **7**, 2216-2225.

[3] Anamika Shah, S.R. and Singh, A. (2017) Mathematical and Computational Study of Blood Flow through Diseased Artery. *International Journal of Computer Science*, **5**, 1-6.

[4] Shah, S.R., Mahesh and Arya, S. (2024) Optimizing Cardiovascular Health: Ayurvedic Insights into Blood Flow through Normal and Stenosed Arteries. *International Journal of AYUSH*, **13**, 18-35.

[5] Udupa, M.C., Saha, S. and Natarajan, S. (2025) Study of Blood Flow Patterns in a Stenosed Artery through the Combined Effect of Body Acceleration and Generalized Womersley Solution. *Scientific Reports*, **15**, Article No. 1845. https://doi.org/10.1038/s41598-025-85566-2

[6] Shah, S.R., Siddiqui, S.U. and Singh, A. (2015) Mathematical Modelling and Analysis of Blood Flow through Diseased Blood Vessels. *International Journal of Engineering and Management Research*, **5**, 366-372.

[7] Singh, S. and Shah, R.R. (2010) A Numerical Model for the Effect of Stenosis Shape on Blood Flow through an Artery Using Power-Law Fluid. *Advance in Applied Science Research*, **1**, 66-73.

[8] Shah, S.R. and Kumar, R. (2017) A Mathematical Approach to Study the Blood Flow through Tapered Stenosed Artery with the Suspension of Nanoparticles. *DEStech Transactions on Engineering and Technology Research*, **1**, 1-6. https://doi.org/10.12783/dtetr/amsm2017/14809

[9] Shah, S.R. (2013) A Mathematical Model for the Analysis of Blood Flow through Diseased Blood Vessels under the Influence of Porous Parameter. *Journal of Biosciences*

and Technology, **4**, 534-541.

[10] Singh, A. and Shah, S.R. (2024) Influence of Transverse Magnetic Field on Steady Blood Flow in a Stenosed Artery: Numerical and Analytical Insights. *International Journal of Mathematical Archive*, **15**, 1-10.

[11] Kumar, V. and Shah, S.R. (2022) A Mathematical Study for Heat Transfer Phenomenological Processes in Human Skin. *International Journal of Mechanical Engineering*, **7**, 683-692.

[12] Reorowicz, P., Obidowski, D., Klosinski, P., Szubert, W., Stefanczyk, L. and Jozwik, K. (2014) Numerical Simulations of the Blood Flow in the Patient-Specific Arterial Cerebral Circle Region. *Journal of Biomechanics*, **47**, 1642-1651. https://doi.org/10.1016/j.jbiomech.2014.02.039

[13] Khalafvand, S.S., Ng, E.Y., Zhong, L. and Hung, T. (2017) Three-Dimensional Diastolic Blood Flow in the Left Ventricle. *Journal of Biomechanics*, **50**, 71-76. https://doi.org/10.1016/j.jbiomech.2016.11.032

[14] Deplano, V., Knapp, Y., Bailly, L. and Bertrand, E. (2014) Flow of a Blood Analogue Fluid in a Compliant Abdominal Aortic Aneurysm Model: Experimental Modelling. *Journal of Biomechanics*, **47**, 1262-1269. https://doi.org/10.1016/j.jbiomech.2014.02.026

[15] Imai, Y., Omori, T., Shimogonya, Y., Yamaguchi, T. and Ishikawa, T. (2016) Numerical Methods for Simulating Blood Flow at Macro, Micro, and Multi Scales. *Journal of Biomechanics*, **49**, 2221-2228. https://doi.org/10.1016/j.jbiomech.2015.11.047

[16] Blanco, P.J., Müller, L.O., Watanabe, S.M. and Feijóo, R.A. (2016) Computational Modeling of Blood Flow Steal Phenomena Caused by Subclavian Stenoses. *Journal of Biomechanics*, **49**, 1593-1600. https://doi.org/10.1016/j.jbiomech.2016.03.044

[17] Narayan, S.S., Rakshitha, S. and Singh, A. (2025) Blood Flow across Cerebral Aneurysms with Magnetic Field Intervention. *Physics of Fluids*, **37**, Article ID: 031901. https://doi.org/10.1063/5.0252178

[18] Elger, D., Slippy, J., Budwig, R., Khraishi, T. and Johansen, K. (1995) A Numerical Study of the Hemodynamics in a Model Abdominal Aortic Aneurysm (AAA). *Proceedings in ASME Symposium on Biomedical Fluids Engineering*, **212**, 15-22.

[19] Paramasivam, V., Muthusamy, K. and Abdul Kadir, M.R. (2010) Application of Computational Fluid Dynamics in Assessing the Hemodynamics in Abdominal Aortic Aneurysms. 2010 *IEEE EMBS Conference on Biomedical Engineering and Sciences* (*IECBES*), Kuala Lumpur, 30 November-2 December 2010, 32-37. https://doi.org/10.1109/iecbes.2010.5742194

[20] Miah, M.A.K., Hossain, S. and Salehin, S. (2020) Effects of Severity and Dominance of Viscous Force on Stenosis and Aneurysm during Pulsatile Blood Flow Using Computational Modelling. *CFD Letters*, **12**, 35-54. https://doi.org/10.37934/cfdl.12.8.3554

[21] Ojha, M., Cobbold, R.S.C., Johnston, K.W. and Hummel, R.L. (1989) Pulsatile Flow through Constricted Tubes: An Experimental Investigation Using Photochromic Tracer Methods. *Journal of Fluid Mechanics*, **203**, 173-197. https://doi.org/10.1017/s0022112089001424

[22] Lee, K.W. and Xu, X.Y. (2002) Modelling of Flow and Wall Behaviour in a Mildly Stenosed Tube. *Medical Engineering & Physics*, **24**, 575-586. https://doi.org/10.1016/s1350-4533(02)00048-6